

Thermal and Dielectric Behavior of Flexible Polycarbonate/Lead Zirconate Titanate Composite System

P. K. Sain,¹ R. K. Goyal,² A. K. Bhargava,¹ Y.V.S.S. Prasad¹

¹Department of Metallurgical and Materials Engineering, Malaviya National Institute of Technology, Jaipur, India

²Department of Metallurgy and Materials Science, College of Engineering, Pune 411005, India

Correspondence to: P. K. Sain (E-mail: pksfmt@gmail.com), R. K. Goyal (E-mail: rkgoyal72@yahoo.co.in)

ABSTRACT: Polycarbonate (PC)/Lead Zirconate Titanate (PZT) composites were prepared using solution mixing method followed by hot pressing. The volume fraction of PZT particles was varied from 0 to 27.5%. SEM showed good dispersion of PZT in the PC matrix. XRD confirmed the perovskite structure of PZT and amorphous structure of polycarbonate. The dielectric constant of the composites measured at 1 kHz, increased ~3.5-fold compared with pure PC. The modified Lichtenecker equation agreed well with the experimental data. There was no dispersion in the dielectric constant of the composites for the frequency range of 1 kHz to 10 MHz. However, at frequencies higher than 10 MHz significant drop in dielectric constant was observed. The dissipation factor of the composites was found below 0.02. However, above 1 MHz, an abrupt increment in the dissipation factor was observed. © 2013 Wiley Periodicals, Inc. *J. Appl. Polym. Sci.* **2014**, *131*, 39913.

KEYWORDS: amorphous; dielectric properties; morphology; polycarbonates; properties and characterization

Received 17 June 2013; accepted 29 August 2013

DOI: 10.1002/app.39913

INTRODUCTION

The passive components of the printed circuit board (PCB) cover more than 40% area and there have been extensive works to embed the passive component in the microelectronic circuits. Embedding these components in the form of film helps in miniaturizing the electronic circuits as well as reduces the metallic connections and solder joints. Reduction in metallic connections and joints increases the reliability of the electronic circuits due to decreased parasitic signal interference. Among various kinds of passive components, embedded capacitors have been in focus due to its versatile applications and properties including decoupling, filtering, timing, A/D conversion, termination, and energy storage. The development of microelectronic requires decoupling capacitors with high capacitance and very low dissipation factor. Generally, a dissipation factor more than 0.05 is considered high.¹ Therefore, real use of embedded capacitor in microelectronics has given a strategic thrust for developing high performance materials exhibiting high dielectric constant with low dissipation factor, and good stability. Many ferroelectric ceramics exhibit high dielectric constant (i.e., up to 10^3 or more). For example, lead zirconate titanate (PZT), and barium titanate (BaTiO_3) ceramics have high dielectric constant, low coefficient of thermal expansion, and good chemical stability, but they have drawbacks of brittleness and high processing temperatures ($>1000^\circ\text{C}$). However, some ceramic-based systems

having lower sintering temperature ($<820^\circ\text{C}$) with good microwave dielectric properties² have been prepared but still not compatible for embedded technology.

To overcome the difficulties associated with ceramics, ceramic-filled polymer composites have been perused as candidate materials for embedded capacitor applications.^{3–11} These composite materials are very attractive because their properties can be easily tailored according to application requirements. The advantages of polymer–ceramic composite films are organic package compatibility, high dielectric constant, localized capacitor formability, and good flexibility.^{12,13} It was reported that the content of the ceramic in the polymer matrix should be more than 50 vol % to increase the dielectric constant of the composites ~10 times or higher relative to the polymer matrix. However, the increase in the volume fraction of ceramic results in brittle film, poor adhesion with substrate, and lower strength.¹⁴ Recently, the dielectric constant of the polyetheretherketone (PEEK)⁹ and polymethylmethacrylate (PMMA)¹⁰ based polymer composites with (~65 vol %) BaTiO_3 was increased approximately 14-fold and 24-fold, respectively. This indicates that the dielectric constant of the composite strongly depends on the type and nature of the polymer matrix. The PZT [$\text{Pb}(\text{Zr}_x\text{Ti}_{1-x})\text{O}_3$; $0 \leq x \leq 1$] particles has been studied as filler with various polymer matrices like nylon 66, polyvinylidene fluoride (PVDF), PMMA etc. and showed encouraging dielectric properties.^{15–19}

Table I. Composition of the PC/PZT Composites

Composite sample	PZT content in the PC matrix by	
	wt %	vol %
C-0	0	0
C-10	10	1.77
C-20	20	3.91
C-30	30	6.52
C-50	50	13.99
C-60	60	19.61
C-70	70	27.51

However, to the best of our knowledge, PZT-filled polycarbonate (PC) composite was not studied, yet. The PC is an industrially important thermoplastic and it has potential applications as a dielectric material with dimensional stability over wide range typically -55°C to 125°C . Moreover, PC exhibits low dissipation factor, high reliability, good toughness, low cost, but low dielectric constant (~ 3), whereas PZT is having high dielectric constant (~ 1000) with high Curie temperature ($\sim 360^{\circ}\text{C}$).^{20–22} In view of this, PC/PZT composites were prepared using solution method followed by hot pressing. To ensure flexibility of the composite films, the maximum loading of PZT powder was kept at about 27.5 vol % (or 70 wt %). The dielectric properties of the composites were studied as a function of PZT content and frequency. The experimental results were also compared with the various existing theoretical models. The dielectric constant of composite increased up to 12 with 27.5 vol % of PZT. Dielectric constant and dissipation factors were almost independent of frequency up to ~ 10 MHz and beyond 10 MHz showed some dependency.

EXPERIMENTAL

Materials

Commercial polycarbonate (PC) was used as matrix. PZT powder (average particle size $0.85\ \mu\text{m}$) was donated by M/s Sparkler Ceramic Private Limited, Bhosari, Pune. According to the supplier, its dielectric constant in polarized state is about 1105. Commercially available tetrahydrofurane (THF) was used as solution medium for mixing of PZT in the PC matrix using ultrasonic bath followed by magnetic stirring.

Composite Preparation

Polycarbonate based composites with varying amount of PZT particles were prepared by mixing them ultrasonically followed by magnetic stirring in THF medium. First, weighed amount of PZT was suspended in THF and subjected to sonication treatment for 30 min to ensure the breaking of agglomerates and finally to achieve uniform dispersion of PZT powder in the THF. Following this, weighed amount of PC granules were added slowly in the properly dispersed PZT/THF suspension with concurrent stirring and heating at $\sim 80^{\circ}\text{C}$. Stirring and heating were maintained till the viscous composite mass was obtained. The viscous composite mass was drawn in the form of thin film by rolling it on a cleaned glass plate. This thin film

then dried in a vacuum oven at 110°C for 15 h. From these films, PC/PZT composite pellets (diameter of 13 mm) were prepared using laboratory size hot press unit (15 ton manual hot and cold press, Kimaya Engineers). The samples were heated with an average heating rate of $7^{\circ}\text{C}/\text{min}$ under a pressure of 45 MPa to a maximum temperature of 240°C . After a soaking period of 20 min, the samples were cooled to a temperature of $\sim 50^{\circ}\text{C}$, so that, the sample could be ejected easily. Composites containing 10, 20, 30, 50, 60, and 70 wt % of PZT powder were prepared. The volume percent of PZT particles (Table I) for selected weight percent in PC matrix was determined from the relation given as in eq. (1);²³

$$V_f = W_f / \left[W_f + W_m \left(\rho_f / \rho_m \right) \right] \quad (1)$$

where V_f is the volume fraction, W_f is weight fraction and ρ_f is the density of the filler (PZT). ρ_m is the density of the matrix (PC).

Characterizations

The theoretical density (ρ_{th}) of the composites was calculated using the rule of mixture (ROM) (eq. (2)), while considering the densities 1.23 g/cc and 7.56 g/cc for PC and PZT, respectively. The experimental density (ρ_{exp}) of the composites was measured using eq. (3) based on Archimedes's principle.

$$\rho_{\text{th}} = \rho_m \cdot (1 - V_f) + \rho_f \cdot V_f \quad (2)$$

$$\rho_{\text{exp}} = [W_{\text{air}} / (W_{\text{air}} - W_{\text{medium}})] \cdot \rho_{\text{medium}} \quad (3)$$

where ρ_m and ρ_f are the densities of PC matrix and PZT, respectively. W_{air} and W_{medium} are the weight of the sample in air and ethanol medium, respectively. The ρ_{medium} is the density of the ethanol medium (i.e., 0.789 g/cc in present case).

X-ray diffraction (XRD) (X'Pert PRO PANalytical) analysis was carried out for the PZT powder and PC/PZT composites. Scanning electron microscopy (SEM) (JEOL: JSM 6010 LV) operated at 20 kV was used to investigate the distribution of PZT particles in the PC matrix. For SEM study, the samples were fractured and coated with a thin layer of platinum using sputter coater. Differential scanning calorimetry (DSC 204F1 Phoenix) was carried out for as received PC, treated PC and PC-PZT composite from 28°C to 300°C with $15^{\circ}\text{C}/\text{min}$ heating rate. Nitrogen atmosphere was used while carrying out DSC. For measuring dielectric properties, both surfaces of the samples were coated with thin layer of silver paste. The dielectric constant was determined using a Wayne Kerr Electronics precision impedance analyzer (6515B, UK) at frequencies varying from 1 kHz to 15 MHz at ambient temperature. The conductivity (σ) and dielectric constant were evaluated by the relations $\sigma = Z/S/t$ and $\epsilon = Ct/\epsilon_0 S$ respectively, where Z is the impedance, S is the surface area, t is the thickness of the dielectric material, C is the capacitance and ϵ_0 is the permittivity of free space (8.854×10^{-12} F/m). Dissipation factor was obtained directly from the instrument.

RESULTS AND DISCUSSION

Theoretical density and experimental density of the composites are shown in Figure 1. The density of the composite increased with increasing PZT content. This is due to the higher density

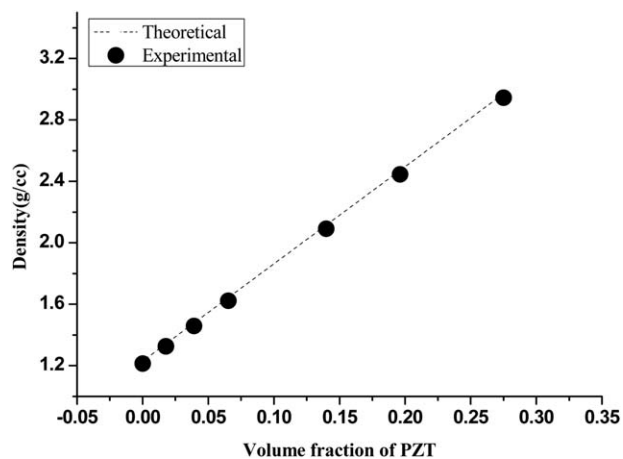


Figure 1. Theoretical and experimental densities of the PC/PZT composite system.

of PZT than that of PC. The experimental densities were almost very close to those of theoretical densities. This shows that the prepared samples are almost porosity free. Figure 2 shows the SEM image of as received PZT powder. It can be seen that the average particle size of PZT powder is below $1\ \mu\text{m}$ which is in agreement with the particle size ($0.85\ \mu\text{m}$) reported by the supplier. Figure 3 shows the SEM images of the composites containing 30 wt % [Figure 3(a)] and 70 wt % [Figure 3(b)] PZT powder. It can be seen that the dispersion of PZT particles is almost uniform in the PC matrix. The pores or porosity is also not found in both composites indicating that the composites are free from porosity as confirmed from density measurement. It is also interesting to see that there is good adhesion between the PZT particles and PC matrix. However, the aggregates of PZT particles can also be seen.

Figure 4 shows the XRD pattern for as received PZT powder. It is apparent from Figure 4 that PZT shows XRD peaks at about $2\theta = 21.8^\circ, 31.1^\circ, 38.3^\circ, 44.4^\circ, 50.2^\circ, 55.3^\circ, 64.9^\circ, 69.1^\circ, 73.6^\circ,$

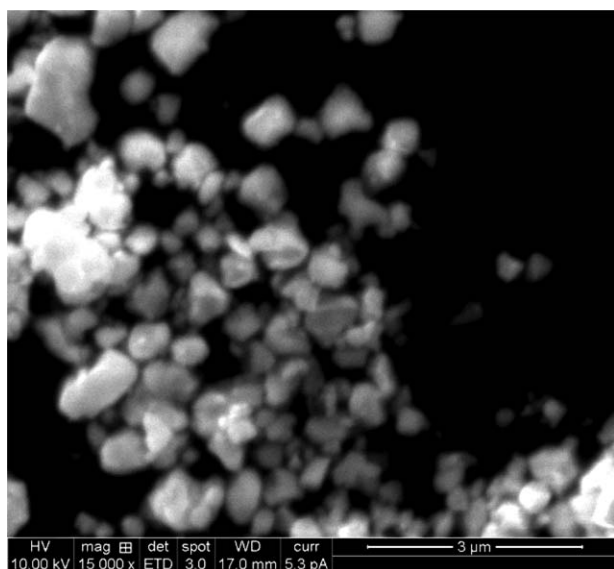


Figure 2. SEM image of PZT powder.

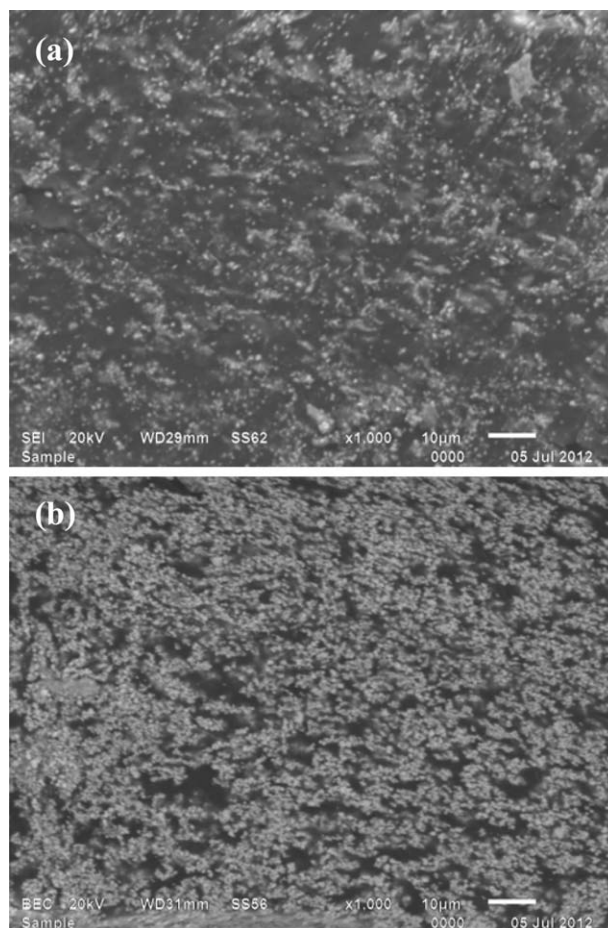


Figure 3. SEM images of PC/PZT composites containing (a) 30 wt% PZT and (b) 70 wt% PZT at magnification of $\times 1000$.

etc. The reflections shows that PZT has rhombohedral [Ref., PDF # 732022 for $\text{Pb}(\text{Zr}_{0.58}\text{Ti}_{0.42})\text{O}_3$] unit cell in perovskite structure (ABO_3 type). In this unit cell all cations and anions slightly moved with respect to their equilibrium position in the cubic perovskite structure and hence possess permanent dipole moment in the [111] direction. (In rhombohedral phase,

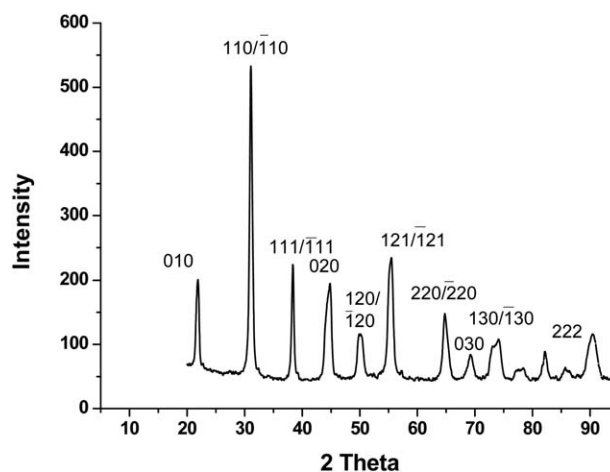


Figure 4. XRD pattern of as received PZT powder.

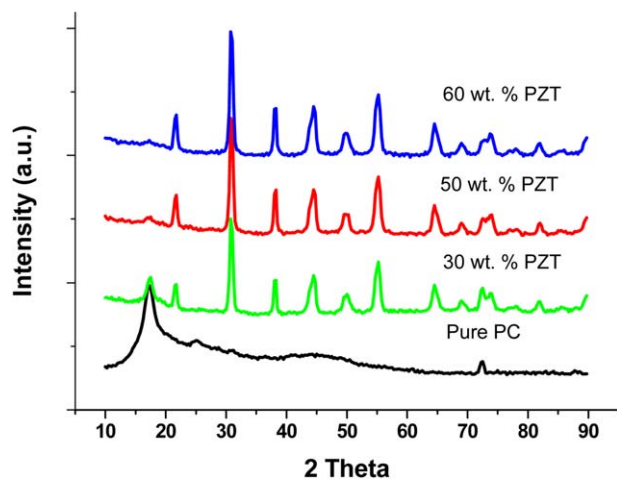


Figure 5. XRD patterns of pure PC and its composites containing 30, 50, and 60 wt % PZT. [Color figure can be viewed in the online issue, which is available at wileyonlinelibrary.com.]

the unit cell distorts along the [111] direction).²² XRD patterns for pure PC and its composite containing 30 wt %, 50 wt %, and 60 wt % PZT are shown in Figure 5. Pure PC shows a broad peak at $2\theta = \sim 17.2^\circ$ indicating that it has amorphous structure. In comparison to pure PZT and PC, the XRD pattern of the PZT and PC in the composites has no obvious differences. However, the intensity of the amorphous halo of the PC matrix is suppressed due to its decreased volume fraction with increasing volume fraction of PZT in the composites.

Figure 6 shows the DSC traces for PC (as received), treated PC (after treating with THF) and a PC-PZT composite having 6.5 vol % (30 wt %) of PZT. It can be seen that as received PC shows a sharp step change at around 149°C which might be correlated to the glass transition temperature (T_g). As received PC does not exhibit any indication for melting point (an endothermic peak would be expected somewhere in between 230 and 250°C). In the cases of treated PC and PC-PZT composite the sharp endothermic peaks were observed which can be correlated to their melting points, however the sharp step changes for T_g were not observed. The absence of melting point peak and pres-

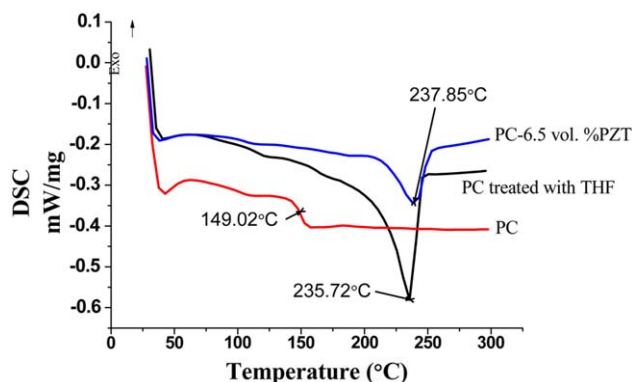


Figure 6. The DSC traces of as received PC, treated PC with THF, and PC-PZT composite. [Color figure can be viewed in the online issue, which is available at wileyonlinelibrary.com.]

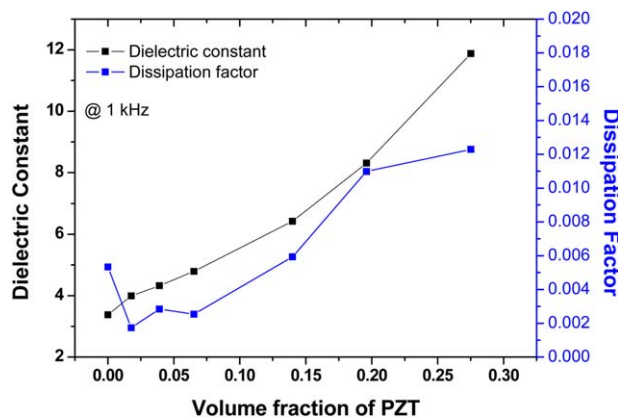


Figure 7. Variation in dielectric constant and dissipation factor of the composite (at 1 kHz) as a function of volume fraction of PZT powder. [Color figure can be viewed in the online issue, which is available at wileyonlinelibrary.com.]

ence of sharp step change at T_g in as received PC indicating that it has mainly amorphous structure which only goes from solid state to flow (beyond T_g the segmental mobility of molecular chains starts) state and hence does not exhibit any sharp melting indication. The DSC traces for treated PC and PC-PZT composites indicate that the crystalline structure is developed after solution treatment and particle incorporation. While solution treating the polymer chains are separated with negligible connections between them. As the solvent gradually evaporates, the concentration increases and chains start to come closer and interact with each other favouring the crystallization to some extent. Incorporation of fillers (PZT in present case) also affects the degree of crystallinity as they may work as the nucleation promoters/inhibitors depending upon the compatibility of particle with matrix polymer. The observations for amorphous and semi-crystalline PC are also in support with the previous work where the PC was treated with acetone in which the amorphous PC did not show any sharp peak for melting point and shown a sharp step change for T_g .²⁴ In case of PC-PZT composite the melting point is slightly shifted to the higher temperature side which may be attributed to the increased crystalline domain embedded in the amorphous region or strong interfacial bonding between PC and PZT which increased interfacial energy and finally the melting point slightly increased. The reduced enthalpy in case of PC-PZT composite might be due to reduced wt % of PC (70 wt % with 30 wt % PZT).

Figure 7 shows the variation in dielectric constant and dissipation factor of the composite as a function of volume fraction of PZT. The dielectric constant and the dissipation factor of the PC measured at 1 kHz were found to be 3.37 and 0.005, respectively. As expected, the dielectric constant of the composites increased with increasing PZT content. This increase in dielectric constant is due to the higher dielectric constant of PZT than that of PC. The dielectric constant is increased approximately to 12 (3.5-fold compared with pure PC) for the composite containing 27.5 vol % (70 wt %) of PZT. This is in agreement with the results reported by Goyal et al.¹⁷ for the PVDF/PZT composites. In the present case of PC-PZT, the

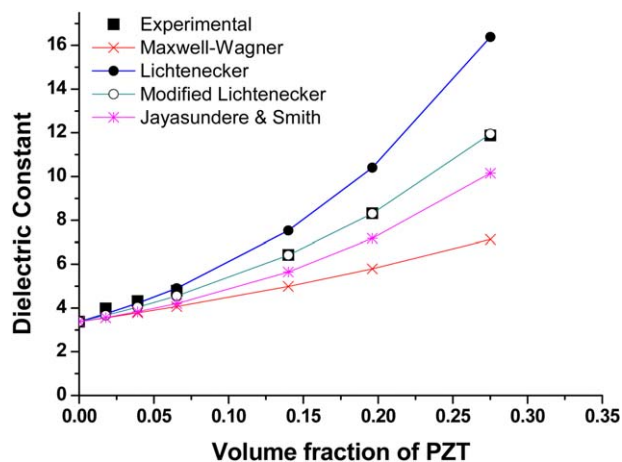


Figure 8. Dielectric constant versus volume fraction of PZT and their correlation with theoretical models. [Color figure can be viewed in the online issue, which is available at wileyonlinelibrary.com.]

dissipation factor is at much better side (below 0.02) than reported for PVDG/PZT composite (compared at almost same filler loading), which is significant from the application point of view. Slight increase in the loss factor at higher loading of PZT can be attributed to the increased interfacial polarization, which increases ionic contribution in polarization mechanism. In Figure 8, the experimental dielectric constant of the composites is correlated with the values predicted from several theoretical models (eqs. (4–7)).

Lichtenecker (eq. (4)), modified Lichtenecker (eq. (5)), Jayasundere and Smith model (eq. (6)), and Maxwell-Wagner (eq. (7)) are used to correlate the dielectric constant of the composites. The modified Lichtenecker equation correlates nicely the experimental data over complete range of PZT content.

$$\log \varepsilon = V_f \log \varepsilon_f + (1 - V_f) \log \varepsilon_m \quad (4)$$

$$\log \varepsilon = \log \varepsilon_f + (1 - k) V_f \log (\varepsilon_f / \varepsilon_m) \quad (5)$$

$$\varepsilon = \frac{(V_m \varepsilon_m) + (V_f \varepsilon_f) * [3\varepsilon_m / (\varepsilon_f + 2\varepsilon_m)] * [1 + \{3V_f(\varepsilon_f - \varepsilon_m)\} / \{\varepsilon_f + 2\varepsilon_m\}]}{V_m + V_f * [3\varepsilon_m / (\varepsilon_f + 2\varepsilon_m)] * [1 + \{3V_f(\varepsilon_f - \varepsilon_m)\} / \{\varepsilon_f + 2\varepsilon_m\}]} \quad (6)$$

$$\varepsilon = \varepsilon_m * \left[\frac{\{2\varepsilon_m + \varepsilon_f + 2V_f(\varepsilon_f - \varepsilon_m)\}}{\{2\varepsilon_m + \varepsilon_f - V_f(\varepsilon_f - \varepsilon_m)\}} \right] \quad (7)$$

where ε , ε_m , and ε_f are the dielectric constants of the composite, PC matrix, and PZT, respectively. In eq. (5), k is an empirical fitting constant for the composites. Its value for most well-dispersed polymer/ceramic composites is about 0.3.^{9,25,26} In present case, $k = 0.20$ correlates the data nicely which is in agreement with the results reported in previous study.⁹ It is to be noted that the experimental data for the full range loading was correlated well the modified Lichtenecker equation indicating that the composites were almost porosity free, PZT particles are strongly bonded with PC (also favoring by DSC analysis of PC-PZT) matrix and perfectly distributed. As apparent from Figure 2 the morphology of PZT particle is not perfect spherically. This might be the probable reason why Jayasundere-Smith and Maxwell-Wagner equations are underestimated the data.³

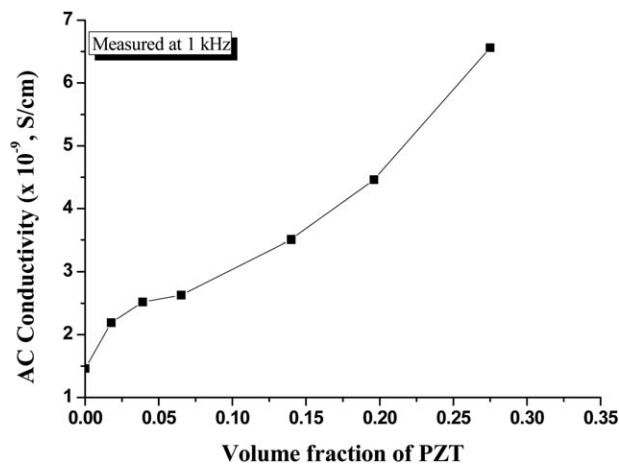


Figure 9. Variation in AC conductivity of PC/PZT composite, measured at 1 kHz, as a function of PZT volume fraction.

Figure 9 shows the alternating current (AC) conductivity of the composites. It increases slightly with increasing volume fraction of PZT. However, the highest electrical conductivity of the composites is 7×10^{-9} S/cm which indicates that composites are insulating. Figure 10 shows the dielectric constants for the pure PC and its composites measured at frequencies varying from 1 kHz to 15 MHz. The dielectric constant for PC/PZT composites are almost frequency independent. The composite is a heterogeneous system which shows anomalous type dielectric constant. The term anomalous dispersion describes a type of variation of dielectric constant with frequency which can be produced by a number of different physical mechanisms.²⁷ Various types of polarization mechanism which contribute to the dielectric constant of a material are electronic polarization, atomic/molecular/ionic polarization, orientation type polarization, and interfacial polarization. Pure PC and its composites show very good stability with frequency up to 10 MHz. However, beyond 10 MHz the dielectric constant decreases probably due to the transition of polarization mechanism (probably from molecular/dipolar to ionic). The work by Das et al.¹⁶ confirms the

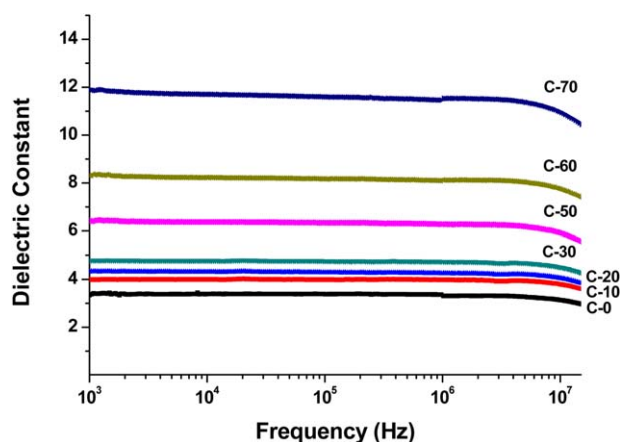


Figure 10. Variation in dielectric constant of PC and its composites, as a function of frequency. [Color figure can be viewed in the online issue, which is available at wileyonlinelibrary.com.]

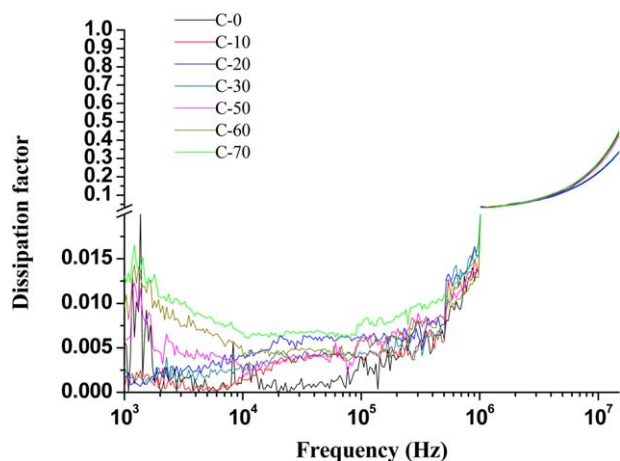


Figure 11. Dissipation factor of composites, as a function of frequency. [Color figure can be viewed in the online issue, which is available at wileyonlinelibrary.com.]

frequency independent behavior of relative permittivity (dielectric constant) for PZT within the studied frequency range which suggests that the decreasing trend should be due to PC. Similar trend for PC at higher frequency (beyond 1 MHz) also confirmed by previous works.^{28,29} The work by Chanmal et al.³⁰ also reported such type of behavior in PVDF at 10 MHz frequency which suggests that the phenomenon (related to some kind of relaxation) which decreases the dielectric constant should be closely related and similar in all polymeric materials. As the percentage of PZT was increased in the PC matrix, the decreasing trend increased with increasing content beyond 10 MHz. This may be ascribed to the increased ionic polarization at interface. Figure 11 shows the dissipation factor of pure PC and its composites as a function of frequency. It was noted that the dissipation factor of the composites is reasonably good and remained below 0.02. In the frequency range of 1 kHz to 100 kHz, dissipation factor decreases for almost all the composites. More than 100 kHz, it increases gradually and above 1 MHz it increases abruptly. This increase at higher frequency may be attributed to unmatched relaxation of interfacial ionic polarization or may be related to some kind of relaxation phenomenon as discussed above. The induced interfacial polarization between PC and PZT or other dielectric relaxations expected at higher frequencies fails to rapidly follow the direction of applied field and contributing loss part increases.

CONCLUSIONS

The flexible polymer matrix composites based on polycarbonate (PC) as matrix and PZT (0–27.5 vol %) as filler were successfully prepared using solution method followed by hot pressing. SEM showed that the dispersion of PZT particles is almost uniform in the PC matrix. According to XRD pattern, the PC showed a broad peak at $2\theta = \sim 17.2^\circ$ indicating that it has amorphous structure and PZT has perovskite structure. DSC along with XRD analysis confirmed the induced crystallinity after solution treating PC with THF. The dielectric constant of the composites increased approximately 3.5-fold with 27.5 vol % (or 70 wt %) PZT. In addition to this, a low dissipation fac-

tor (i.e., < 0.02 @ 1 kHz) is the important achievement of this study. Modified Lichtenecker equation correlates very well the data. Limiting volume fraction of PZT ensures the flexibility of the composite system. The AC conductivity of the composites increases slightly with increasing PZT content in the matrix but the composites still remain insulating. To the best of our knowledge, such flexible composite films with good dielectric constant and low dissipation factor may be useful as matrix for three-phase composite systems in future.

ACKNOWLEDGMENT

Author P. K. Sain acknowledges Garima Kedawat and Jyoti, Research Scholars at the department of Physics, University of Rajasthan, and Archana, M. Tech., at COEP, Pune for their help in characterizing his samples. Authors are thankful to Dr. Vibhat Saraswat, department of Physics, Banasthali, Niwai, Rajasthan for providing DSC facility. Authors further extend their sincere thanks to Prof. K. B. Sharma, Principal Subhodh PG college, Jaipur for providing Impedance analyser facility.

REFERENCES

- Ulrich, R. K.; Schaper, L. W. *Integrated Passive Component Technology*; Hoboken, NJ: IEEE Press, Wiley-Interscience, **2003**.
- Zhou, D.; Wang H.; Pang, L. X.; Randall, C. A.; Yao, X. *J. Am. Ceramic Soc.* **2009**, *92*, 2242.
- Cho, S. D.; Lee, S. Y.; Hyun, J. G.; Paik, K. W. *J. Mater. Sci.* **2005**, *16*, 77.
- Yoon, J. R.; Han, J. W.; Lee, K. M. *Trans. Electrical Electronic Mater.* **2009**, *10*, 116.
- Xu, J.; Wong, C. P. *J. Electronic Mater.* **2006**, *35*, 1087.
- Hyun, J. G.; Lee, S.; Cho, S. D.; Paik, K. W. *Electronic Components Technol. Conference.* **2005**, 1–7.
- Rao, Y.; Ogitali, S.; Kohl, P.; Wong, C. P. *Int. Symp. Adv. Compos. Packaging Mater.* **2000**, 32.
- Xu, J.; Bhattacharya, S.; Moon, K. S.; Lu, J.; Englert, B.; Wong, C. P. *Electronic Components Technol. Conf.* **2006**, 1520.
- Goyal, R. K.; Madav, V. V.; Pakankar, P. R.; Butee, S. P. *J. Electron. Mater.* **2011**, *40*, 2240.
- Goyal, R. K.; Katkade, S. S.; Mule, D. M. *Compos. Part B.* **2013**, *44*, 128.
- Liang, S.; Chong, S.; Giannelis, E. *Proceeding of the 48th Electronic Component and Technology Conference.* **1998**, 171.
- Vrejoiu, I.; Pedarnig, J. D.; Dinescu, M.; Gogonea S. B.; Bauerle, D. *Appl. Phys. A.* **2002**, *74*, 407.
- Kakimoto, A.; Takahashi, A.; Tsurumi, T.; Hao, J.; Li, L.; Kikuchi, R.; Miwa, T.; Oono, T.; Yamada, S. *Mater. Sci. Eng. B.* **2006**, *132*, 74.
- Rao, Y.; Ogitali, S.; Kohl, P.; Wong, C. P. *J. Appl. Polym. Sci.* **2002**, *83*, 1084.
- Nayak, B.; Mansingh, A.; Machwe, M. K. *J. Mater. Sci.* **1999**, *25*, 749.

16. Das-Gupta, D. K.; Doudhty, K. *Thin Solid Films* **1998**, *158*, 93.
17. Goyal, R. K.; Kulkarni, A. B. *J. Phys. D: Appl. Phys.* **2012**, *45*, 1.
18. Gregorio, R.; Cestari, M.; Bernardino, F. E. *J. Mater. Sci.* **1996**, *31*, 2925.
19. Runt, J.; Galgoci, E. C. *J. Appl. Polym. Sci.* **1984**, *29*, 611.
20. Mugford, C. E. Report No. 68007. An Assessment of the Long Term Capacitor Requirements for Static Power Conversion Equipments, Signal Research and Development Establishment, *Ministry of Technology*. **1969**, 1–10.
21. Tohge, N.; Takahashi, S.; Minam, T. *J. Am. Ceram. Soc.* **1991**, *74*, 67.
22. Jin, L. Thesis. Broadband Dielectric Response in Hard and Soft PZT: Understanding Softening and Hardening Mechanisms. Swiss Federal Institute of Technology, Lausanne, Switzerland. **2011**, 4–5.
23. Goyal, R. K.; Samant, S. D.; Thakar, A. K.; Kadam, A. *J. Phys. D: Appl. Phys.* **2010**, *43*, 1.
24. Handbook of Polycarbonate Science and Technology, Hudgin, D. E.; Bendler, J. T., Eds.; Marcel Dekker, p 295.
25. Kota, R.; Ali, A. F.; Lee, B. I. *Microelectronic Eng.* **2007**, *84*, 2853.
26. Sonoda, K.; Juuti, J.; Moriya, Y.; Jantunen, H. *Compos. Struct.* **2010**, *92*, 1050.
27. Murphy, B. J.; Morgan, S. O. *Bell System Tech. J.* **1937**, 493.
28. Mujahid, M.; Singh, P.; Srivastava, D. S.; Gupta, S.; Avasthi, D. K.; Kanjilal, D. *Radiat. Measure.* **2004**, *38*, 197.
29. Mujahid, M.; Srivastava, D. S.; Avasthi, D. *Radiat. Phys. Chem.* **2011**, *80*, 582.
30. Chanmal, C. V.; Jog, J. P. *Xpress Polym. Lett.* **2008**, *2*, 294.